HiSST: International Conference on
High-Speed Vehicle Science Technology
26–29 November 2018, Moscow, Russia

Nonlinear flutter of curved composite panels in high speed flow

Xiaomin An[1], Yixiang Liu[2], Baiyi Qi[3]

Abstract

Nonlinear aeroelastic behaviors of two cylindrical composite panels are studied in a transonic flow of Ma=0.96. The cylindrical shell structure is modeled by an assemblage of flat triangular elements and the large displacement is described by a parameterization of the orthogonal matrix. Euler equation is solved by an upwind flux splitting scheme and a dual-time technology to obtain nonlinear aerodynamic loads. Based on a loosely coupling procedure, nonlinear aeroelastic responses of the two cylindrical composite panels are computed. The nonlinear characteristics, such as large displacement in structure, shock wave motions and flow separation in aerodynamic field are analyzed.

Keywords: *nonlinear aeroelasticity, composite structure, geometric nonlinearity, panel flutter*

Nomenclature

[1] *School of Astronautics, Northwestern Polytechnical University, Xi'an, 710072, China. E-mail: frank805@nwpu.edu.cn*
[2] *School of Astronautics, Northwestern Polytechnical University, Xi'an, 710072, China. E-mail: 562041409@qq.com*
[3] *School of Astronautics, Northwestern Polytechnical University, Xi'an, 710072, China. E-mail: 1746694610@qq.com*

Latin

$\mathbf{T}$ – Transform matrix between local and global frame

$\mathbf{K}$ – Global Stiffness matrix

$\mathbf{M}$ – Global mass matrix

$\boldsymbol{F}$ – Global force

$\bar{\mathbf{U}}$ – fluid variables

$\bar{\mathbf{Q}}$ – Inviscid flux

$\Delta \boldsymbol{d}$ – Displacement increment vector

$\ddot{\boldsymbol{d}}$ – Acceleration vector

$\dot{\boldsymbol{d}}$ – Velocity vector

dt – real-time step of the aerodynamic sover

Δt – time step of the structural sover

$d\boldsymbol{S}$ – outer normal area vector of the control surface

$\boldsymbol{V}$ – velocity of the control volume

K_f – Non-dimensional flutter frequency

Ma – Mach number

w/h –The normalized vertical displacements of the panel centre

Greek

δ_n – Greek symbol

Ω – Moving control finite volume

$d\tau$ – Pseudo time step of the aerodynamic sover

λ – Non-dimensional dynamic pressure

Subscripts

i – The internal variable of the structure

s – The structural variable

a - The aerodynamic variable

n+1– Step number

T – Tangent variable

σ – Geometric variable

1. Introduction

Aeroelastic analysis of the panel, especially for flat panel flutter problems in supersonic flow regime, has been investigated for many decades, and a large number of studies can be found. Dowell et al. [1-3], Gordnier and Visbal [4], Mei [5] and some other distinguished researcher have dedicated a lot to this region. However, the exposed skin of the structure of the aerospace industry always have a certain curvature, and composite materials, which have high stiffness and strength-to-weight ratio, are being widely used. Consequently, the static aeroelastic deformation will arise and the aeroelastic behaviors will present a more complex characteristic under aerodynamic loading. Dowell [2, 3] studied the flutter amplitude and boundary of 2D and 3D streamwise curved plates by a nonlinear Galerkin analysis and quasi-steady aerodynamic theory, and pointed out that the static aerodynamic loading significantly affects the flutter boundary. Gray and Mei [5, 6] presented a finite element approach to determine the nonlinear flutter characteristics of 3D thin laminated composite panels using the 3rd piston theory and von Karman large-deflection plate theory. Castro et al. [7] presented a modified piston theory to predict the aeroelastic response of laminated composite stiffened panels, and the results showed that the stiffener base significantly affects the panel aeroelastic behavior. However, there are few published works on the nonlinear aeroelastic behavior of curved composite panels in transonic flow regime.

This paper will do some research for simulating nonlinear aeroelastic behaviours of cylindrical composite panels. The concrete results, static aeroelastic deformation, non-periodic oscillations and chaos are obtained. The nonlinear characteristics, such as large displacement in structure, shock wave motions and flow separation in aerodynamic field are analyzed.

2. Modeling

The cylindrical shell structure, as shown in Fig.1, is modeled by an assemblage of flat triangular elements in the local coordinate system.

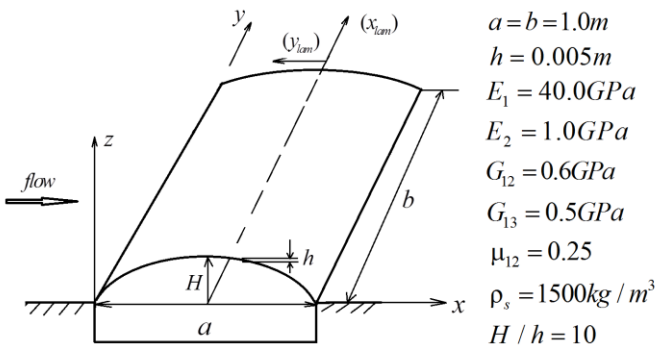

Fig. 1 Geometry of a cylindrical composite panel

By introducing a parameterization of the orthogonal matrix to represent large rotation, the global displacements and inter forces can be determined. Through virtual work and the relations of the differentiation, the tangent stiffness matrix is obtained as:

$$\mathbf{K}_T = \mathbf{T}^T \mathbf{K}_l \mathbf{T} + \mathbf{K}_\sigma \tag{1}$$

The governing equation for the shell structure is then derived as

$$\mathbf{M}\ddot{\boldsymbol{d}}_{s,n+1} + \mathbf{K}_{T,n}\Delta \boldsymbol{d}_s = \boldsymbol{F}_{s,n+1} - \boldsymbol{F}_{i,n} \tag{2}$$

In order to obtain unsteady aerodynamic load, an implicit course of the dual-time technology is introduced to solve the Euler equation as

$$\Omega \frac{d\bar{\mathbf{U}}}{d\tau} + \frac{3\Omega^{n+1}\bar{\mathbf{U}}^{n+1} - 4\Omega^{n}\bar{\mathbf{U}}^{n} + \Omega^{n-1}\bar{\mathbf{U}}^{n-1}}{2dt} + \bar{\mathbf{Q}}^{n+1} = 0 \tag{3}$$

The inviscid flux $\bar{\mathbf{Q}}$ and can be obtained by the upwind flux splitting scheme. The Geometric Conservation Law (GCL) is introduced to solve for the moving finite volume as follows:

$$\Omega^{n+1} = \frac{4}{3}\Omega^{n} - \frac{1}{3}\Omega^{n-1} + \frac{2\Delta t}{3}\int \boldsymbol{V}\cdot d\boldsymbol{S} \tag{4}$$

The above two equations (2) and (3) are connected by Farhat's second order loosely coupling procedure, as shown in Fig. 2.

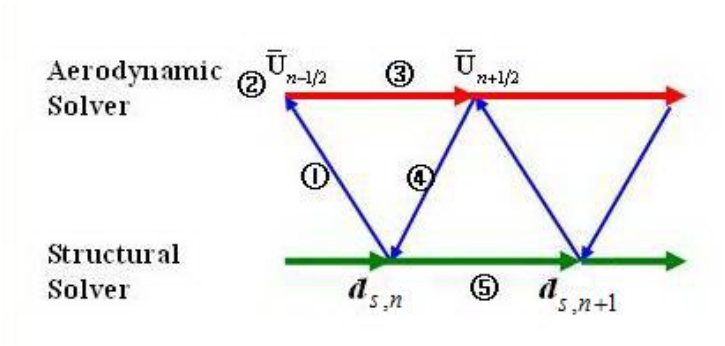

Fig. 2 Flowchart of second order loosely coupled procedure

Following are details about the major steps of the coupled procedure:

STEP 1: Predict the structural displacement at time-step $n+1/2$ by the structural motion at n step, and transfer the predicted motion to the fluid system as $\boldsymbol{d}_{a,n+1/2}$, that is

$$\boldsymbol{d}_{a,n+1/2} = \boldsymbol{d}_{s,n} + \frac{\Delta t}{2}\dot{\boldsymbol{d}}_{s,n} \tag{5}$$

STEP 2: Update the position of the fluid grids by Transfinite Interpolation (TFI) technique and compute the new control finite volume by Eq. 4.

STEP 3: Solve Eq. 3 to obtain the loads on the aerodynamic surface $\boldsymbol{F}_{a,n+1/2}$.

STEP 4: Convert the aerodynamic loads $\boldsymbol{F}_{a,n+1/2}$ into structure element as $\boldsymbol{F}_{s,n+1/2}$, and compute the equivalent loads by

$$\boldsymbol{F}_{s,n+1} = 2\boldsymbol{F}_{s,n+1/2} - \boldsymbol{F}_{s,n} \tag{6}$$

STEP 5: Solve Eq. 2 by Newmark algorithm to get the structural motion at time-step $n+1$.

3. Results and Discussion

3.1. Nonlinear transient response of a spherical composite shell

The nonlinear transient response of a spherical laminated composite shell under a uniform internal pressure $q = 1.0 \times 10^4 N/m^2$, which has been analyzed by Kundu [8] and Almeida [9], is adopted to verify the nonlinear structural dynamic solution. The geometry of the simply supported spherical panel is shown in Fig. 6, and the structural properties are: $a = 0.5m$, $R = 5m$, $E_1 = 181GPa$, $E_2 = 10.3GPa$, $G_{12} = G_{13} = 7.17GPa$, $\mu_{12} = 0.28$, $G_{23} = 3.58GPa$ and $\rho_s = 1600kg/m^3$. The panel consists of 8 equal thickness layers with $[0°/\pm 45/90°]_S$. The total thickness of the shell is given by the relations $a/h = 50$.

The structure of the shell is modeled by a 512 triangle elements and 289 nodes, and the time step is set to $\Delta t = 0.0001s$. The time step and the number of nodes are equal to those adopted by Kundu [8] and Almeida [9]. The normalized vertical displacements of the panel centre are obtained and compared with the results of Kundu and Almeida, as can be seen in Fig. 4. For the case of a/h = 50, the computed results in the present work are in good agreement with those given by the references.

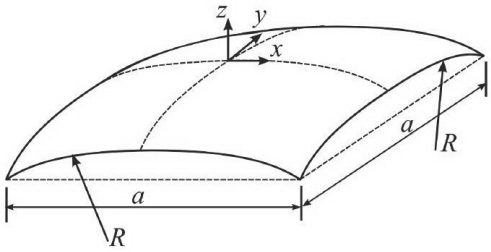

Fig. 3 Geometry of a spherical shell

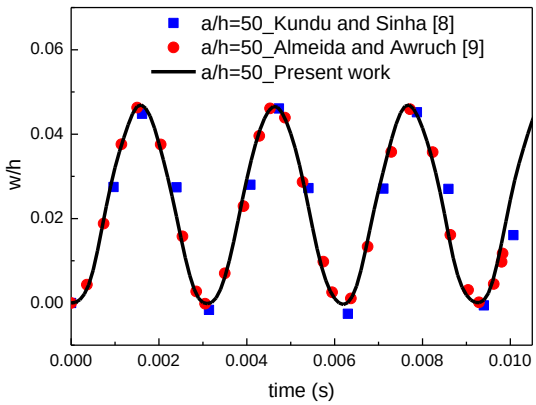

Fig. 4 The normalized vertical displacements of the panel center

3.2. Unsteady aerodynamic solver for AGARD CT5 test

AGARD CT5 unsteady flow test is introduced to validate the present aerodynamic solver. The unsteady motion of NACA0012 airfoil is defined as $\alpha(t)=0.016°+2.51°\sin(2\times0.0814t)$. The flow condition is Ma=0.755, and the axis position is at 0.25 chord. The flow grid is constructed by O-type grid consisting of 121×80 points. The computed results of lift and moment are presented in Fig.5 (a) and Fig.5 (b), respectively. Clearly, comparing with the results of Batina [10], the numerical results obtained by the present work are much closer to the experimental values [11]. The comparisons demonstrate that the present aerodynamic solver has accurate prediction capabilities.

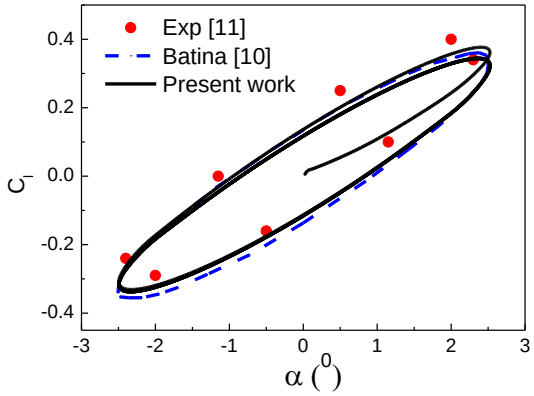

(a) Lift coefficient vs. angle of attack;

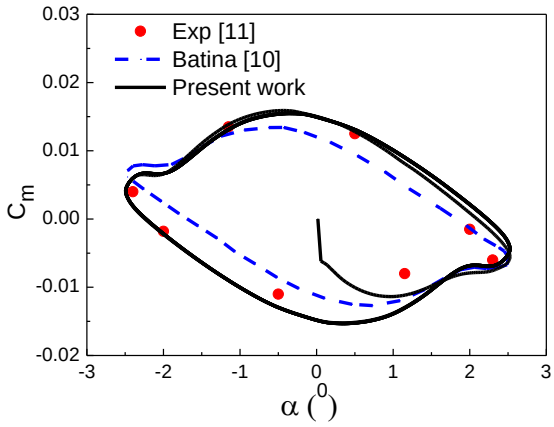

(b) Moment coefficient vs. angle of attack

Fig. 5 Results of unsteady CT5 test

3.3. Two-dimensional flat panel flutter validation

A flexible panel of length a, thickness h, and mass density ρ_s as shown in Fig. 6 is investigated to validate the coupled procedure at Ma=1.2. The panel's characteristics are: h/a=0.002, mass ratio $\mu_s=\rho_\infty a/\rho_s h=0.1$, Poisson's ratio $\nu=0.3$ and modulus of elasticity $E_s=7.0\times10^{10}$. Two different boundary conditions are considered at both edges of the panel: simply supported case and clamped case (they are simplified as "S" and "C" in the figure). The flow is constructed by H-type grid consisting of 161×41 points, and the finite element model composes of 21 beam elements.

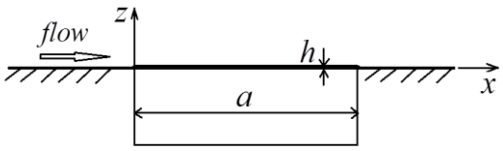

Fig. 6 Geometry of a two-dimensional flat panel

Figures 7 (a) and (b) show the non-dimensional limit cycle oscillation amplitude and flutter frequency values of the present work and those given by Dowell [2], Gordnier and Visbal [4] at x/a=0.75 of Ma=1.2. Obivously, either the simply supported condition or the clamped condition, the results of flutter amplitude obtained by the present work are compared well with those computed by Gordnier and Visbal. For the case of simply supported condition, the amplitude values given by Dowell are slightly higher because of the linearized potential theory was adopted in his work. With regard to the flutter frequency, the results of the present work compare very well with those given by Gordnier and Visbal, except for the case of clamped condition at λ=150.

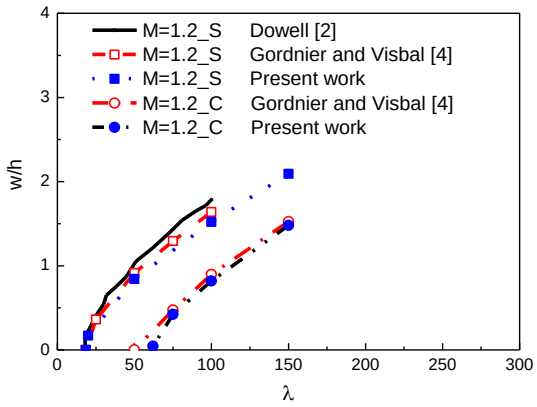

(a) Limit cycle oscillation amplitude vs. dynamic pressure;

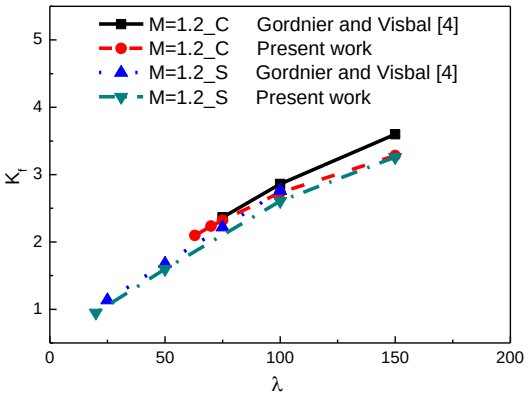

(b) Flutter frequency vs. dynamic pressure

Fig. 7 Aeroelastic response for 2D panel at x/a=0.75 of *Ma*=1.2

3.4. Nonlinear aeroelastic analysis of curved laminated composite panels

The developed program is applied to calculate nonlinear aeroelastic responses of the two cylindrical, composite panels, which have ply angles as [0°/90°/0°/90°/0°] and [45°/-45°/45°/-45°/45°] in a transonic flow of Ma=0.96.

With a wide range of dynamic pressure, the static aeroelastic deformation is always observed, and the deformation of the panel of ply [45°/-45°/45°/-45°/45°] is larger than the other case with the growth of the dynamic pressure as shown in Fig.8.

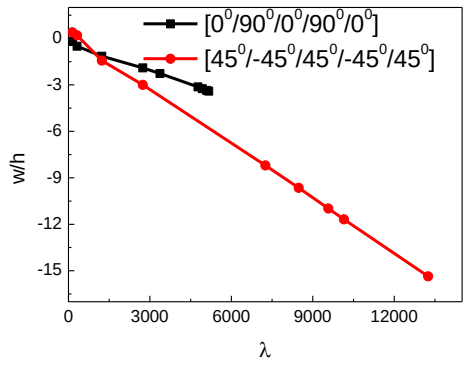

Fig. 8 Static deflection vs. dynamic pressure

Fig. 9 shows the amplitude of the oscillation under several dynamic pressure. It can be found that the amplitude augments with the increase of the dynamic pressure. Moreover, the amplitudes of the oscillations are more than 17.5 times the thickness of the panel, and the dynamic pressure corresponding to the oscillation of the ply [45°/-45°/45°/-45°/45°] case is much higher than that of the other one.

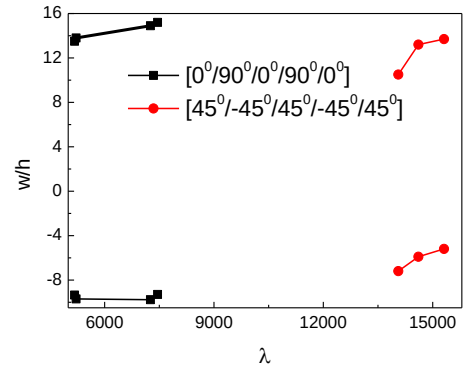

Fig. 9 Amplitude vs. dynamic pressure

In the case of [0°/90°/0°/90°/0°], there are non-periodic high-frequency oscillations under λ=5176 (Fig.10) and λ=7453 (Fig.11). When the dynamic pressure gets a certain larger value, there will be a small separate region behind the shock wave on the end part of the panel and it travels with the movement of the panel.

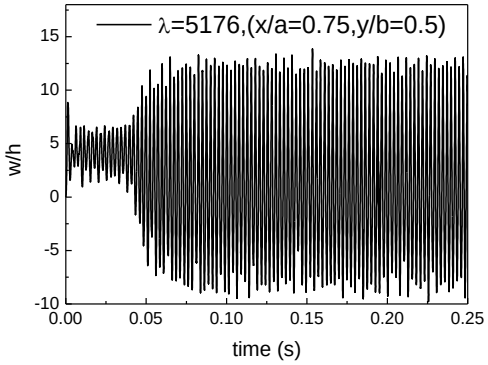

Fig. 10 Aeroelastic response at λ=5176

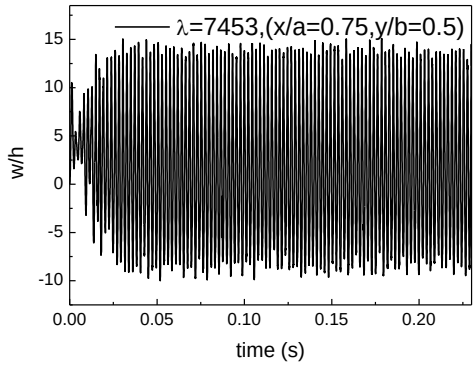

Fig. 11 Aeroelastic response at λ=7453

For the panel of ply [45°/-45°/45°/-45°/45°], the oscillations are somewhat sensitive and complicated with a quite low-frequency cycle. Take λ=14057 as an instance, Fig. 12 displays the time-histories of the oscillations. It appears as quasi-periodic. In addition, the dominant first frequency of the oscillation is quite small, about 16.9Hz, even smaller than the first-order modal frequency of the structure (about 93Hz).

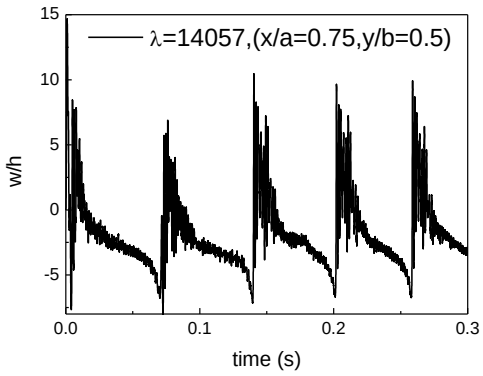

Fig .12 Aeroelastic response at λ=14057

Fig. 13 and Fig. 14 show the Mach number and displacement distribution on the surface of the panel at the moment of the positive and negative peaks of the process, respectively. It can be found that the vortex always exists behind the shock wave on the end part of the panel along the flow direction at the two moments, and the position of the shock wave vary with the motion of the panel. Because the value of the pressure in the supersonic region decreases, the displacements in the z-direction on the back part of the panel are always positive, as seen in Fig. 14. Furthermore, the displacement distribution is non-symmetrical about y/b=0.5 as a result of the non-symmetrical lay angle.

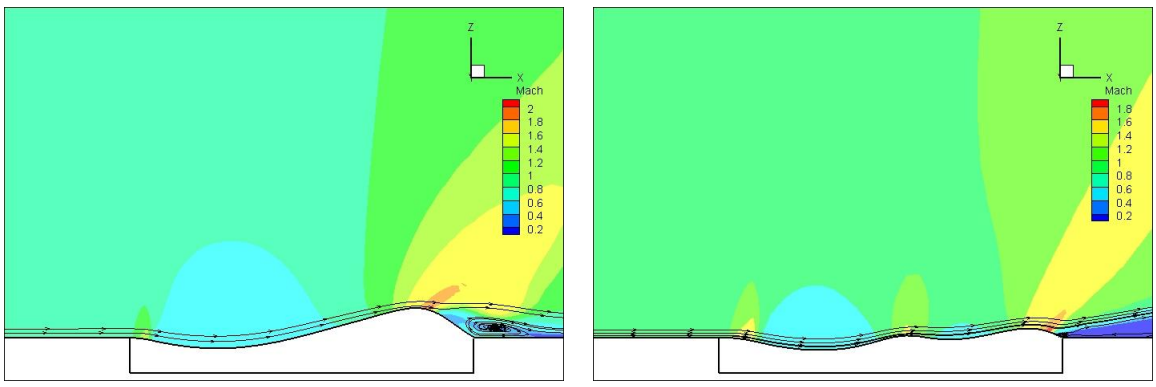

(a) t=0.259s, positive peak of the oscillations; (b) t=0.327s, negative peak of the oscillations

Fig. 13 Mach number distribution at the section y/b=0.5 at λ=14057

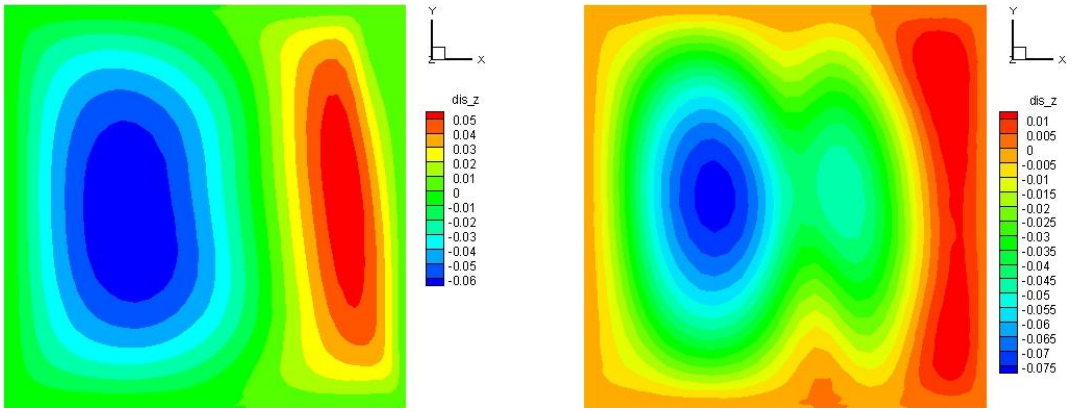

(a) t=0.259s, positive peak of the oscillations; (b) t=0.327s, negative peak of the oscillations

Fig. 14 Displacement distribution in the z-direction on the surface of the panel at λ=14057

With the increase of the dynamic pressure, when λ=14608 (Fig.15) and λ=15312 (Fig.16), the trajectories will change to chaotic patterns after several quasi-periodic cycles.

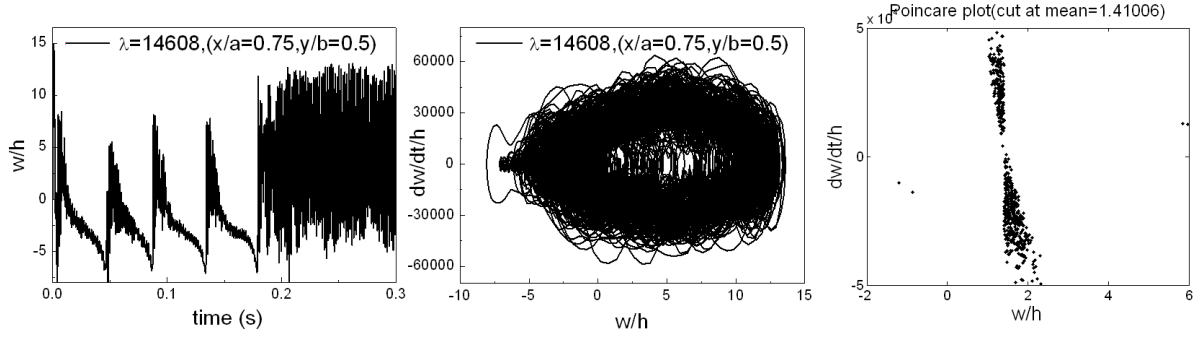

(a) Time-histories of the oscillation; (b) Phase portrait; (c)Poincare map;

Fig .15 Aeroelastic response at λ=14608

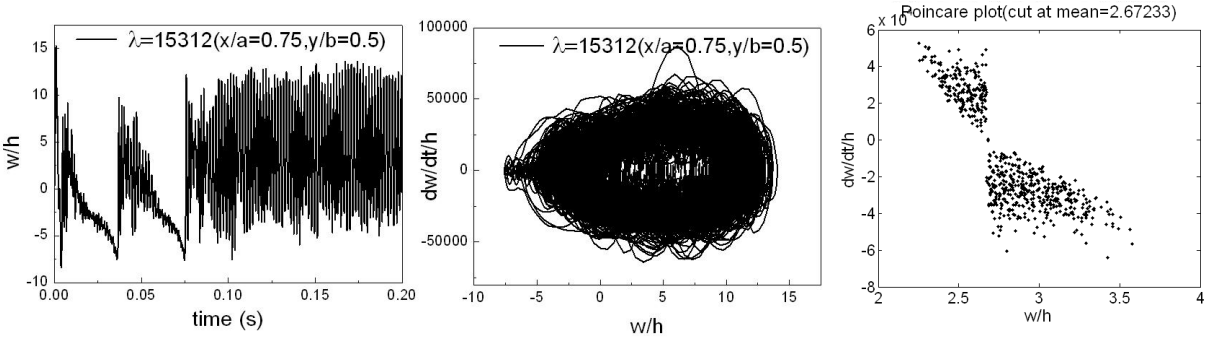

(a) Time-histories of the oscillation; (b) Phase portrait; (c)Poincare map;

Fig .16 Aeroelastic response at λ=15312

4. Conclusions

For the different value of non-dimensional dynamic pressure, the static aeroelastic deformation, non-periodic oscillation and chaotic results are obtained. With a wide range of the dynamic pressure, the deformation of the panel of ply [45°/-45°/45°/-45°/45°] is larger than the other one. When the dynamic pressure gets to a certain larger value, there will be a separated region on the end part of the panel and it travels with the movement of the panel.. The oscillation of the panel of ply [0°/90°/0°/90°/0°] appear as high-frequency non-periodic vibrations. The oscillation of the panel of ply [45°/-45°/45°/-45°/45°] is somewhat sensitive and complicated with a quite low-frequency cycle.

Besides, the flutter dynamic pressure of the two panels are always relatively large, and the amplitude of the oscillations are more than 17.5 times the thickness of the panel.

References

- Journal article

1. Dowell, E. H., Thomas, J .P, Hall, K.C.: Transonic limit cycle oscillation analysis using reduced order aerodynamic models, AIAA 2001-1212 (2001)
2. Dowel, E. H.: Nonlinear flutter of curved plates, AIAA J 7: 424-431 (1969)
3. Dowel, E. H.: Nonlinear flutter of curved plates. II AIAA J 8:259-261(1970)
4. Gordnier, R ..E, Visba,l M.R.: Development of a three-development of a three-dimensional viscous aeroelstic solver for nonlinear panel flutter. Journal of Fluids and Structures 16, 497-527 (2002)
5. Gray, J.C.E., Mei, C.: Large-amplitude finite element flutter analysis of composite panels in hypersonic flow. AIAA J 31, 1090-1099(1993)
6. Mei, C.: A Finite-Element Approach for Nonlinear Panel Flutter, AIAA J 15, 1107-1110(1977)
7. Castro, S., Guimarães, T., Rade, D.: Flutter of stiffened composite panels considering the stiffener's base as a structural element, Composite Structures, 140, 36-43 (2016)
8. Kundu, C., Sinha K.: Nonlinear transient analysis of laminated composite shells. Journal of Reinforced Plastics and Composites, 25, 1129-1147 (2006)
9. Almeida S., Awruch M.: Corotational nonlinear dynamic analysis of laminated composite shell structures, Proceeding of PACAM XI, 11th Pan-American Congress of Applied Mechanics - PACAM XI January 04-08, 2010, Foz do Iguaçu, PR, Brazil.
10. Batina T., Unsteady Euler airfoil solutions using unstructured dynamic meshes, AIAA J 28, 1381-1388(1990)
11. Compendium of Unsteady Aerodynamic Measurements, AGARD R-702(1982)